

2D internal multiple prediction in coupled plane wave domain

Jian Sun, Kristopher A.H. Innanen

ABSTRACT

Internal multiples can be constructed by primary events based on inverse scattering series (ISS) algorithm. More benefits can be achieved in plane wave domain, such as improved numerical accuracy, no large offset artifacts, and less computing time. In view of that, the plane wave domain ISS algorithm can be a promising way to eliminate internal multiples on a full 2D case. We presented 2D internal multiple predictions using ISS algorithm in coupled plane wave domain. The coupled $\tau - p_g - p_s$ transform offers a straightforward approach to obtain the input. Some preliminary results are achieved and further research is ongoing. Be that as it may, those preliminary results still exemplify ISS algorithm in the coupled plane wave domain can provide much more relevant and practical profits.

INTRODUCTION

Multiples attenuation plays an important role in seismic processing because its quality will directly affect the accuracy of seismic imaging and interpretation. Multiples can be identified as two major classes, surface-related multiple and interbred multiple, in the light of the influence of free-surface. Surface-related multiples can be successfully eliminated as its periodic appearance in $\tau - p$ domain and many innovative technologies have been developed. Taner (1980) and Treitel et al., (1982) demonstrated predictive deconvolution can be applied to remove surface-related multiples based on its periodic property. Verschuur (1991) proposed an inverse approach for multiple attenuation using the feedback model and a similar method was described by Weglein et al. (1997) on the strength of inverse scattering series. Liu et al., (2000) presented surface-related multiple attenuation on 2D case in the plane wave domain using the invariant embedding technique. Berkhout and Verschuur (2005, 2006) derived a multiple attenuation method using inverse data processing and Ma et al., (2009) implemented this algorithm in plane wave domain.

However, attenuation of the other classical multiple, internal multiple, is still a giant challenge in seismic data processing even though much considerable progress have been made recently. Kelamis et al. (2002) introduced a boundary-related/layer-related approach to remove internal multiples in the poststack data and CMP domains. Berkhout and Verschuur (2005, 2006) extended the inverse data processing to attenuate internal multiples by considering internal multiples as the suppositional surface-related multiples through the layer-related or boundary-related approach in common-focus-point (CFP) domain. The same algorithm was applied by Luo et al. (2007) by re-datuming the top of the multiple generator, thereby, internal multiples will be transformed to be 'surface-related'. The common ground of those algorithms is that extensive knowledge of subsurface is somewhat required, which is not appropriate in all practical situations, especially for complex land datasets.

Inverse scattering series (ISS) indicated that all possible internal multiples can be reconstructed by primary events (Weglein et al. 1997), and the algorithm is full data driven, which means no subsurface information required and all internal multiples generator will be treated in a stepwise and automatic way (Weglein et al. 1997; D. J. Verschuur and Berkhout 2005). Hernandez and Innanen (2012) implemented ISS algorithm on poststack dataset. 1.5D tests was carried out by Pan and Innanen (2013, 2015) on synthetic, physical modeling dataset in wavenumber pseudo-depth domain on the basis of the version proposed by Innanen (2012). In previous posts, we further analyzed the relationship between pseudo-depth and intercept time on the foundation of Coates et al. (1996) and Nita and Weglein (2009). And the inverse scattering approach was presented more efficiently in the plane wave domain with improved numerical accuracy and reduced large-offset artifacts (Sun & Innanen, 2014, 2015). Consider the complexity of land dataset, 2D internal multiples attenuation is presented with coupled $\tau - p$ transform. Some preliminary predictions are achieved and further analyzed is still ongoing. Even so, those results demonstrate that more potential and practical benefits can be achieved using the inverse scattering series in the coupled plane wave domain.

INVERSE SCATTERING SERIES ALGORITHM

Araujo et al. (1994) and Weglein et al. (1997) demonstrated that the traveltime of multiples can be obtained by summing over those events which satisfy lower-higher-lower relationship. In theory, the algorithm can be expressed as,

$$\begin{aligned}
 & b_{3_{IM}}(k_g, k_s, \omega) \\
 &= \frac{1}{(2\pi)^2} \iint_{-\infty}^{+\infty} dk_1 e^{-iq_1(\varepsilon_g - \varepsilon_s)} dk_2 e^{-iq_2(\varepsilon_g - \varepsilon_s)} \int_{-\infty}^{+\infty} dz e^{i(q_g + q_1)z} b_1(k_g, k_1, z) \\
 &\times \int_{-\infty}^{z-\varepsilon} dz' e^{-i(q_1 + q_2)z'} b_1(k_1, k_2, z') \int_{z'+\varepsilon}^{+\infty} dz'' e^{i(q_2 + q_s)z''} b_1(k_2, k_s, z'') \quad (1)
 \end{aligned}$$

where

$$q_X = \frac{\omega}{c_0} \sqrt{1 - \frac{k_X^2 c_0^2}{\omega^2}}; \quad k_z = q_g + q_s;$$

q_X , are vertical wave numbers associated with the various lateral wave numbers and the reference velocity. z , z' and z'' are the pseudo-depth which satisfy the lower-higher-lower relationship. The input of ISS algorithm is $b_1(k_g, k_s, k_z) = -2iq_s D(k_g, k_s, k_z)$. The left-hand side of equation (1) is inverse Fourier transformed over all three Fourier variables, and the result is added to the original data to attenuate the multiples, normally with an adaptive component to account for small phase and amplitude mismatches between the prediction and the actual multiples.

Bear in mind that the relationship between intercept time and pseudo-depth,

$$k_z z = \omega \tau \quad (2)$$

where, z is the pseudo-depth applied in equation (1), τ is the intercept time of the events.

Combined equation (1) and (2), the plane wave domain ISS algorithm can be described (Coates et al. 1996),

$$b_{3_{IM}}(p_g, p_s, \omega) = \frac{1}{(2\pi)^2} \iint_{-\infty}^{+\infty} dp_1 e^{-i\omega(\tau_{1g}-\tau_{1s})} dp_2 e^{-i\omega(\tau_{2g}-\tau_{2s})} \int_{-\infty}^{+\infty} d\tau e^{i\omega\tau} b_1(p_g, p_1, \tau) \times \int_{-\infty}^{\tau-\epsilon} d\tau' e^{-i\omega\tau'} b_1(p_1, p_2, \tau') \int_{\tau'+\epsilon}^{+\infty} d\tau'' e^{i\omega\tau''} b_1(p_2, p_s, \tau'') \quad (3)$$

where p_g, p_s are the source and receiver horizontal slownesses (which are equal in 1.5D cases) respectively. The time variables τ, τ' and τ'' are intercept time of three events satisfied lower-higher-lower relationship. Figure 1 shows ray-path of primaries and internal multiple, which also indicates the relationship among p_g, p_s, p_1, p_2 in Eq. (3). Note that, the internal multiple indicated in Figure 1 can be easily constructed by those three events, $b_1(p_2, p_s, \tau'')$ in red, $b_1(p_1, p_2, \tau')$ in green, $b_1(p_g, p_1, \tau)$ in blue, as long as $\tau'' > \tau'$ and $\tau > \tau'$. Once the inputs with respect to p_g, p_s, τ are generated, Eq. (3) can be applied to predicted all possible internal multiples.

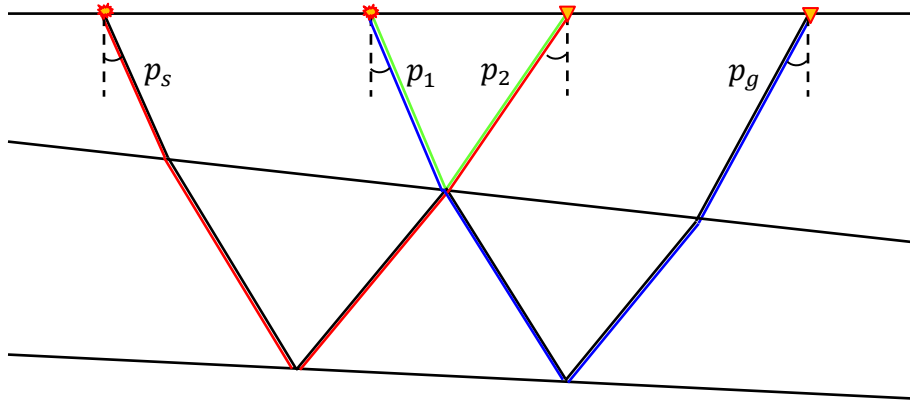


FIG. 1. Ray-path schematic of primaries (red, blue, green) and internal multiple (black)

COUPLED $\tau - p$ TRANSFORM

In practice, $\tau - p$ transform is a useful tool to separate different seismic events by decomposing the seismic matrix into events with respect to intercept time and ray parameter. A traditional $\tau - p$ transform of the wavefield $\Psi(x, t)$ collected with offset x at time t can be described as

$$\psi(p, \tau) = \int \Psi(x, \tau + px) dx \quad (4)$$

where, p is the ray parameter and τ is the intercept time. For a fixed point in plane wave domain, Eq. (4) represents a summation of wavefield along the linear trajectory $t = \tau + px$, and then located it at (p, τ) . The $\tau - p$ transform can also be performed by calculating the integration over offset in frequency domain,

$$\phi(p, \omega) = \int \varphi(x, \omega) e^{i\omega px} dx \quad (5)$$

In $\tau - p$ domain, each trace represents the plane wave arrivals with a fixed angle between ray-path and vertical direction, which can be reflected by different angles of incidence waves. Typical $\tau - p$ transform is performed for a fixed source location (or receiver location) with respect to the offset. Consider multicomponent and multi-coverage data introduced into seismic exploration, $\tau - p$ transform can also be applied with respect to both source and receiver locations at the same time. Liu et al. (2000) applied double $\tau - p$ through offset and source location to suppress surface-related multiples. Stoffa et al. (2006) implemented depth migration using double $\tau - p$ transform with respect to source and receiver position.

Similarly to Eq. (5), double $\tau - p$ transform of the multicoverture data can be considered as the decomposition with respect to source and receiver locations simultaneously in frequency domain, which can be accomplished by the variant slant stacking with a particular phase shift applied over source and receiver respectively (Stoffa et al. 2006). Therefore, the forward double $\tau - p$ transform for a fixed frequency can be expressed as,

$$D(p_s, p_g, \omega) = \iint_{-\infty}^{+\infty} d(x_s, x_g, \omega) e^{+i\omega(p_s x_s + p_g x_g)} dx_s dx_g \quad (6)$$

with the inverse double $\tau - p$ transform as,

$$d(x_s, x_g, \omega) = \iint_{-\infty}^{+\infty} D(p_s, p_g, \omega) e^{-i\omega(p_s x_s + p_g x_g)} dp_s dp_g \quad (7)$$

where, x_s, x_g are the source and receiver location in a same coordinate. p_s, p_g are the horizontal slowness at source location and receiver location respectively. Eq. (6) can also be written as a slant stack, as followed,

$$\widehat{D}(p_s, p_g, \tau) = \iint d(x_s, x_g, \tau + p_s x_s + p_g x_g) dx_s dx_g \quad (8)$$

Eq. (8) indicates that, unlike the conventional $\tau - p$ transform, the double $\tau - p$ transform is the processing of summation along a planar plane instead of a liner trajectory. Eq. (8) also demonstrates the relationship between traveltime t in recorded data and the intercept time τ in double $\tau - p$ transformed gathers,

$$t = \tau + p_s x_s + p_g x_g \quad (9)$$

To further analyze the meaning of τ in double $\tau - p_g - p_s$ domain, we recall the $\tau - p$ mapping method with dip introduced by Ocola (1972) and Diebold and Stoffa (1981). Consider their theory, $\tau - p$ mapping for a fixed source location x_s can be written as

$$t = p_g x + \sum_i z_{si} (q_{si} + q_{gi}) \quad (10)$$

Or, in a case of a fixed receiver location,

$$t = p_s x + \sum_i z_{gi} (q_{si} + q_{gi}) \quad (11)$$

where, t is the travel time and x is the offset. p_s, p_g are horizontal slowness at source and receiver location respectively. q_{si}, q_{gi} are the vertical components of slowness in the

i^{th} layer with respect to source and receiver respectively. z_{si}, z_{gi} are the thicknesses of i^{th} layer below source and receiver location.

In order to implement the $\tau - p$ mapping on CMP gather, Diebold and Stoffa (1981) also introduced a reference point (M), which is located at the midpoint between source and receiver in CMP gather, and applied the $\tau - p$ transform based on the reference point location. The $\tau - p$ mapping with respect to a reference point location can be expressed as

$$t = p_s x_{s-M} + p_g x_{g-M} + \sum_i z_{Mi} (q_{si} + q_{gi}) \quad (12)$$

where, x_{s-M} is the distance between source and the reference point, and x_{g-M} is the distance between geophone and the reference point. p_s, p_g, q_{si}, q_{gi} have the same meaning of Eq. (11). z_{Mi} is the thicknesses of i^{th} layer below the reference point location.

To make an intuitive understanding of Eq. (6), we consider the origin as the reference point. Thus, x_{s-M} and x_{g-M} are converted to the source x_s and receiver x_g locations, respectively (Figure 2). And combine the Eq. (8), (9), (12), we have the intercept time in double $\tau - p$ transformed data (Note that, when $x_s = 0$ and $x_g = 0, t = \tau$),

$$\tau = \sum_i z_i (q_{si} + q_{gi}) \quad (13)$$

Double $\tau - p$ transform can also be related to the conventional slant stack. Liu et al., (2000) implemented 2D $\tau - p$ transform with respect to source location and offset,

$$D(p_d, p_0, \omega) = \iint_{-\infty}^{+\infty} d(x_s, x, \omega) e^{+i\omega(p_d x_s + p_0 x)} dx_s dx \quad (14)$$

After matrix $D(p_d, p_0, \omega)$ obtained, a linear remapping can be applied to calculate data matrix $D(p_s, p_g, \omega)$, with $p_0 = p_g$,

$$D(p_s, p_g, \omega) = D(p_0 - p_d, p_0, \omega) \quad (15)$$

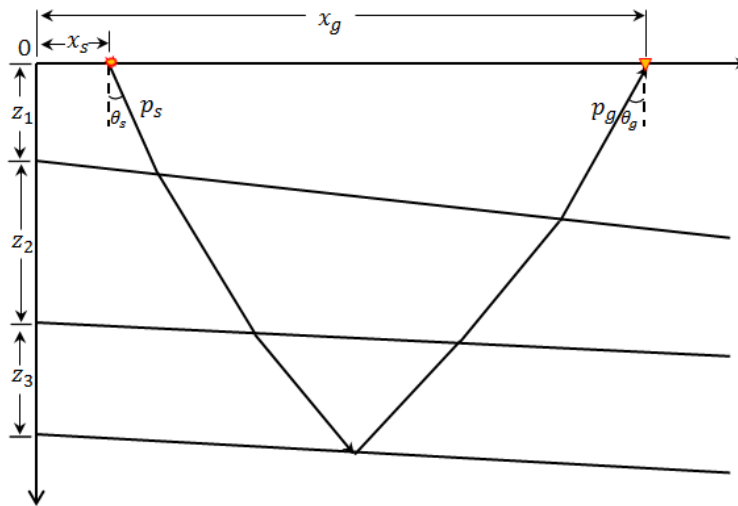


FIG. 2. The schematic diagram of ray-path with a source location of x_s , and recorded at x_g . Here, consider $\theta_s < 0$ and $\theta_g > 0$, then we have $p_s < 0, p_g > 0$.

Figure 3 shows the processing steps of double $\tau - p$ transform. In Figure 3a), a fixed shot record ($x_s = 636m$) included two reflected events is shown. A $\tau - p$ transform with respect to receiver location was implemented first by slant stacking along a linear trajectory of $t = \tau + p_g x_g$ on 3D matrix (x_s, x_g, τ) . A slice matrix (p_g, τ) was extracted from the $\tau - p_g$ transformed data (x_s, p_g, τ) at the same source location ($x_s = 636m$) delineated in Figure 3b). Note that, $x_g = x_s = 636m$, $\tau(p_g = 0) = t(x_g = x_s)$; and $p_g \rightarrow -\frac{1}{c_0}, \tau = t(x_g = 0)$.

Figure 3c) shows the slice matrix (x_s, τ) with a fixed $p_g = 0$. After $\tau - p_g - p_g$ transform completely applied, the slice (p_s, τ_0) with a fixed $p_g = 0$ was extracted and indicated in Figure 3d).

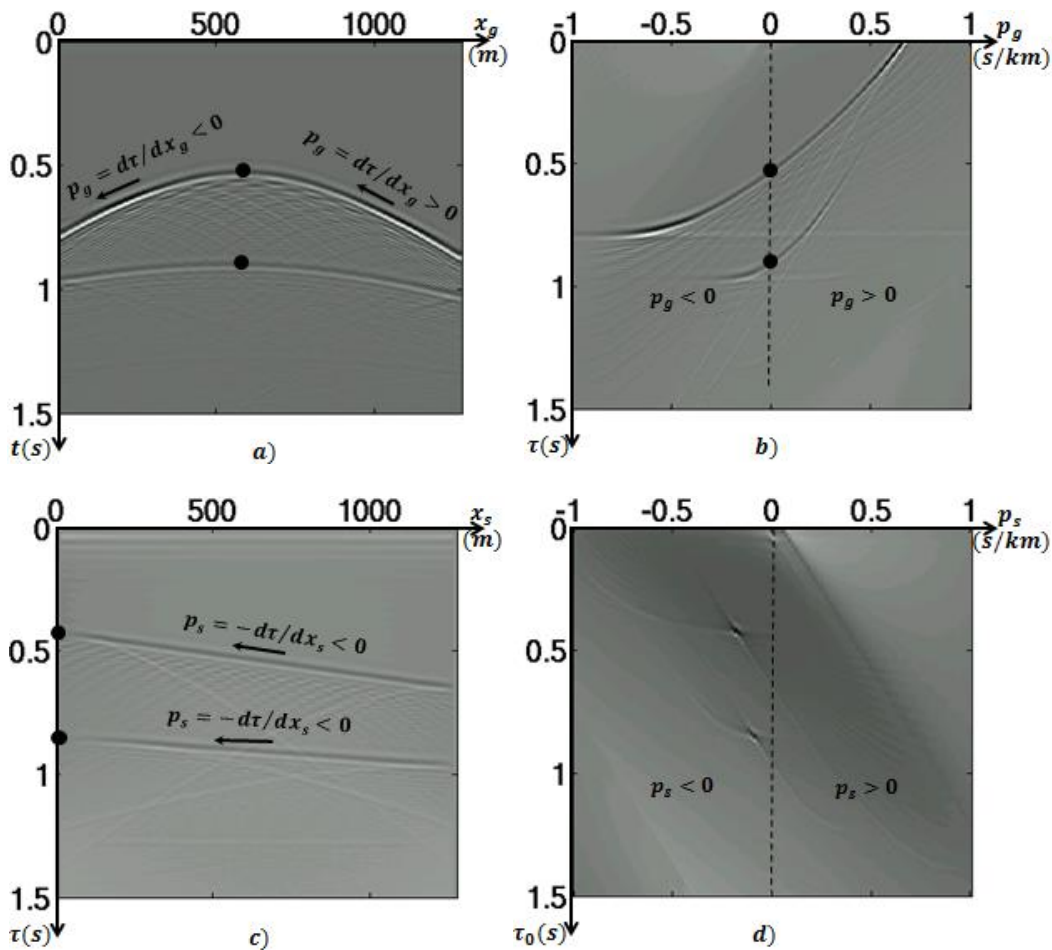


FIG. 3. Procedures of double $\tau - p$ transform. a) Record for a fixed source location, i.e., data matrix (x_g, t) with $x_s = 636m$. b) Reflections in a) mapped into (p_g, τ) domain. c) Common p_g ($p_g = 0$) gather extracted from same data volume showed in b), i.e., data matrix (x_s, τ) . d) Common p_g gather extracted from data volume $D(p_g, p_s, \tau)$, i.e., data matrix (p_s, τ) with $p_g = 0$.

Liu et al., (2000) also indicated that ray parameters of downgoing and upgoing wave are connected and the difference of them is limited, which can be expressed as

$$\left| |p_s| - |p_g| \right| \leq \frac{2 \sin \alpha}{v_{min}} \quad (16)$$

where, α is the maximum dipping angle of layers, v is the velocity. For a flat layer case, $\alpha = 0$, and $p_s = -p_g$. Eq. (16) indicated the matrix (p_s, p_g) for a fixed frequency is bandlimited and diagonal sparse matrix (Figure 4). After $D(p_g, p_s, \tau)$ obtained, 3D volume will be scaled by $-i2q_s$, and treated as the sparse matrix during the prediction.

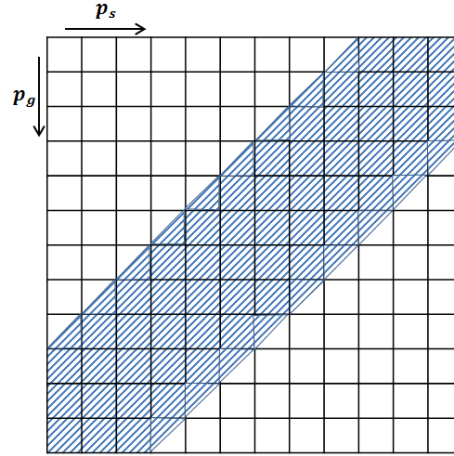


FIG. 4. Diagonal sparse matrix (p_s, p_g) for a fixed frequency

EXAMPLES

To examine the capacity of the ISS algorithm in double plane wave domain, a 3-layer model including two reflectors (Figure 5, one dipping reflector with 8° and one flat reflector) was used to generate the multi-shot wavefields. 128 geophones of 10m intervals were line located at 40m below surface to suppress the ghost. Sources were moving from the first geophone location to the last one, i.e., moving in 10m step, to generate shot gathers at different locations.

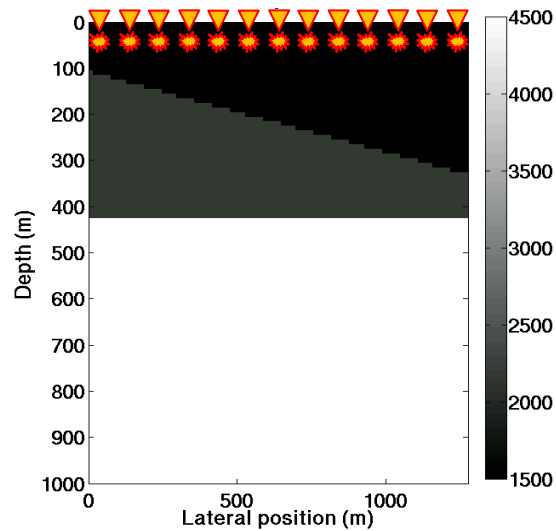


FIG. 5. Velocity model used to generate multi-shot gathers, velocity in upper layer is 1500m/s, velocity in medium layer is 2200m/s, velocity of the lower layer is 4500m/s.

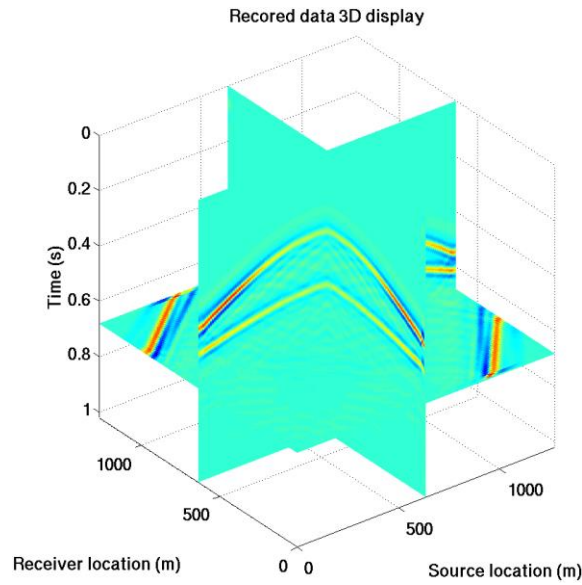


FIG. 6. 3D views of 128 shot gathers in source coordinate, receiver coordinate and time

Figure 6 shows the 3D view of the recorded data. 3 matrices slices, $(x_s = 636m, x_g, t)$, $(x_s, x_g = 636m, t)$ and $(x_s, x_g, t = 0.64s)$, were extracted and displayed in $x_s - x_g - t$ coordinates. Only primaries and internal multiples are included in the data volume. Three shot gathers at location: 310m, 630m and 950m, were extracted and presented in Figure 7a). The first order internal multiples in 3 gathers were indicated by the arrow, and they have different trajectories due to the existed dipping layer. After double $p_s - p_g - \tau$ transform, three common p_s gathers ($p_s = -0.3, 0, 0.3$) are shown in Figure 7b).

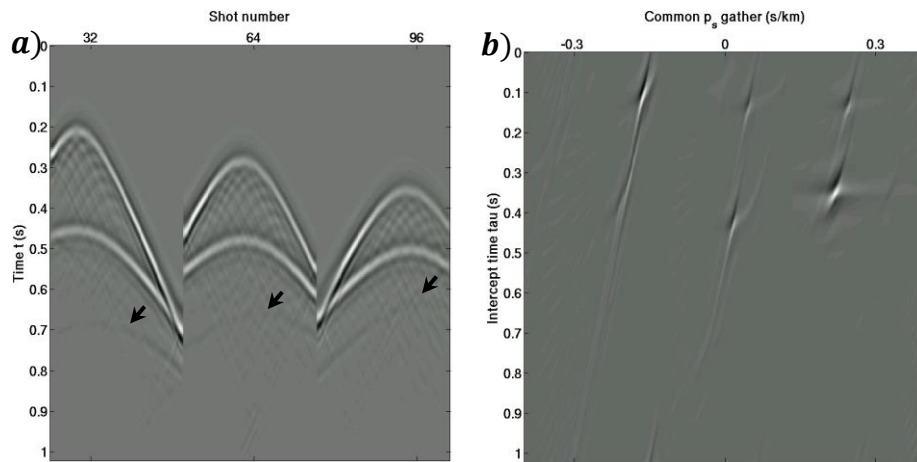


FIG. 7. a) Acoustic finite difference synthetic shot gathers at three locations: **310m, 630m, and 950m**, and 1st order internal multiple is indicated by the arrow. b) Shot gathers in (p_s, p_g, τ) domain and three slices extracted in $p_s = -0.3, 0, 0.3$.

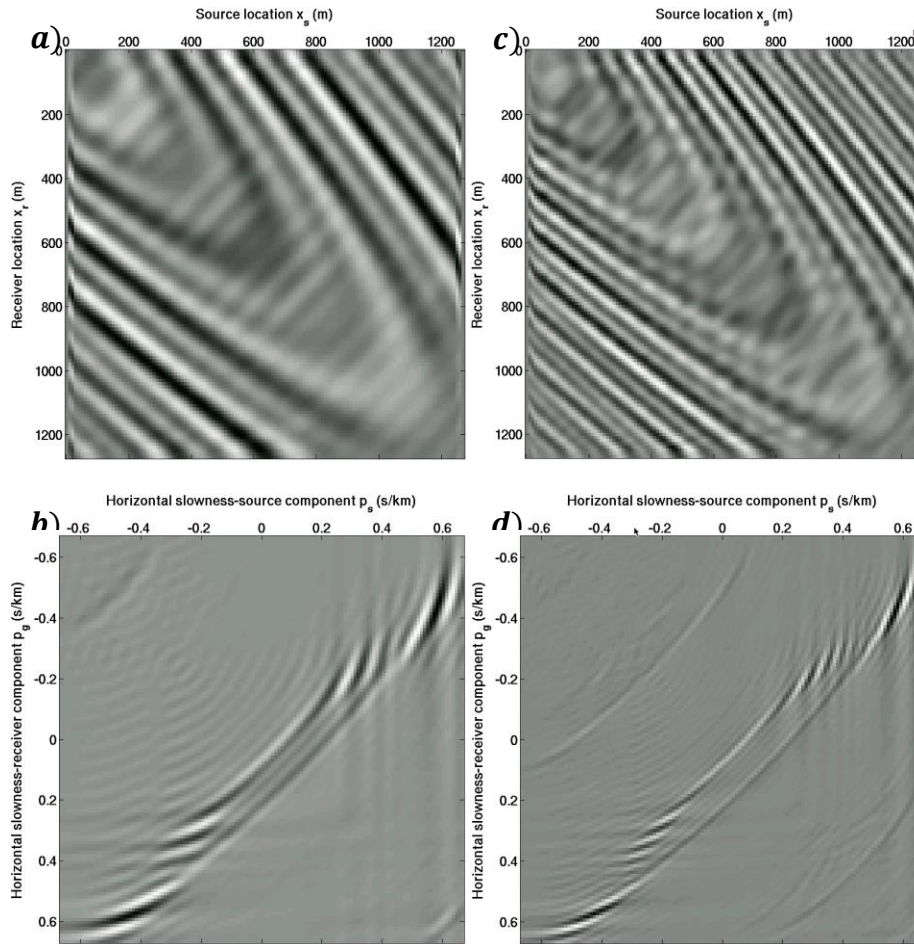


FIG. 8. Fixed frequency data matrices comparison of (x_s, x_g, ω) domain and (p_s, p_g, ω) domain. a) data matrix (x_s, x_g) at 15 Hz. b) data matrix (p_s, p_g) at 15 Hz. c) data matrix (x_s, x_g) at 25 Hz. d) data matrix (p_s, p_g) at 25 Hz.

Figure 8 indicates 15Hz and 25Hz matrices in (x_s, x_g, ω) domain and (p_s, p_g, ω) domain separately. Compared to the main diagonal symmetric of matrices (x_s, x_g) , matrices (p_s, p_g) in double plane wave domain are anti-diagonal symmetry. Particularly worth mentioning is that the energy are more convergence around anti-diagonal in (p_s, p_g, ω) domain, which means the computation burden might be reduced to some extent due to the highly sparse of matrices (p_s, p_g) .

Data volume $D(p_s, p_g, \tau)$ will be scaled by multiplying $-i2q_s$ to achieve the input of ISS algorithm in double plane wave domain, and results are shown in Figure 9. Figure 9a) shows 3 common p_s gathers ($p_s = -0.3, 0, 0.3$), and 3 common p_g gathers ($p_g = -0.3, 0, 0.3$) are delineated in Figure 9b). Figure 9c) and 9d) show the matrix matrices (p_s, p_g) at 15Hz and 25 Hz separately. We can see that input volume $b1(p_s, p_g, \omega)$ is also centered exactly on the anti-diagonal of matrix (p_s, p_g) . Therefore, the input volume will be considered as anti-diagonal sparse 3D matrix in the processing of internal multiple predictions using ISS algorithm.

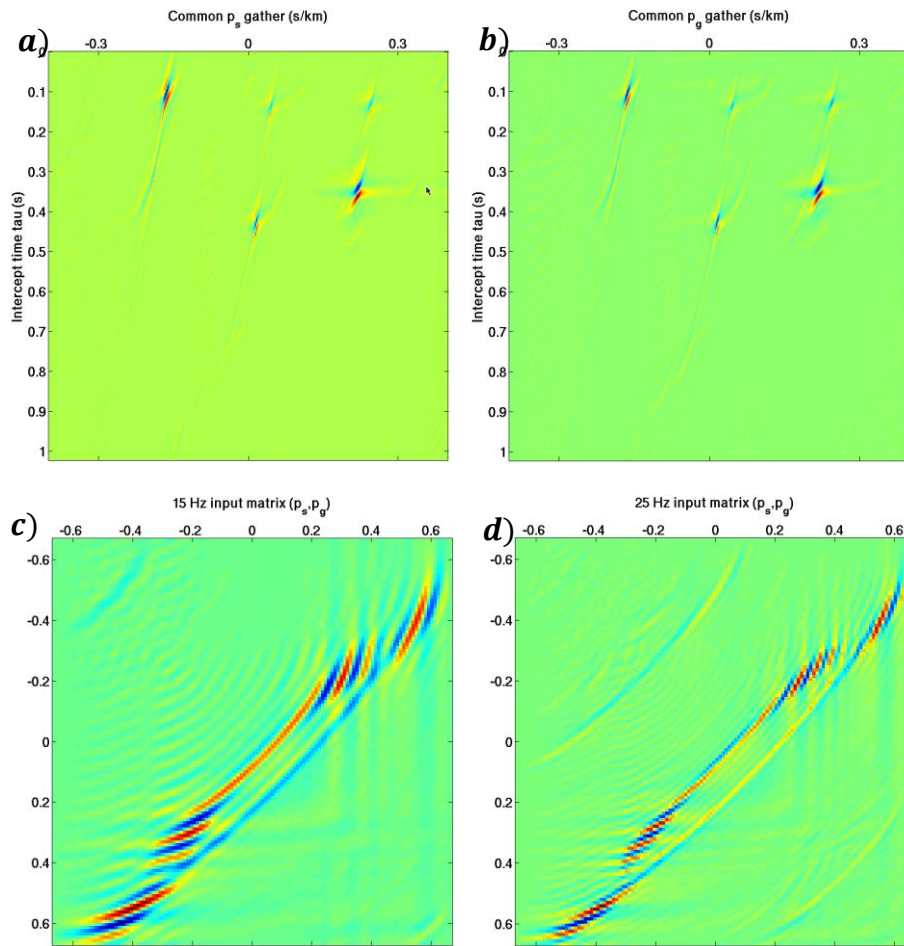


FIG. 9. Input data $(\mathbf{p}_s, \mathbf{p}_g, \tau)$ displays. a) 3 common \mathbf{p}_s gathers ($\mathbf{p}_s = -0.3, 0, 0.3$) extracted from input volume. b) 3 common \mathbf{p}_g gathers ($\mathbf{p}_g = -0.3, 0, 0.3$) extracted from input volume. c) 15 Hz input matrix $(\mathbf{p}_s, \mathbf{p}_g)$. d) 25 Hz input matrix $(\mathbf{p}_s, \mathbf{p}_g)$.

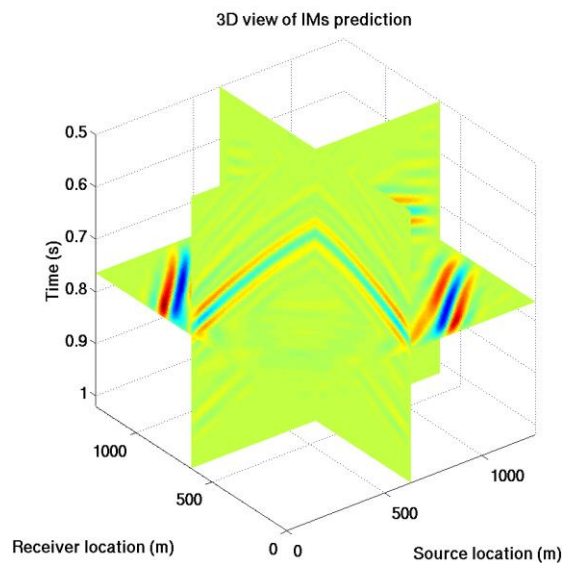


FIG. 10. 3D display of internal multiple predicted dataset

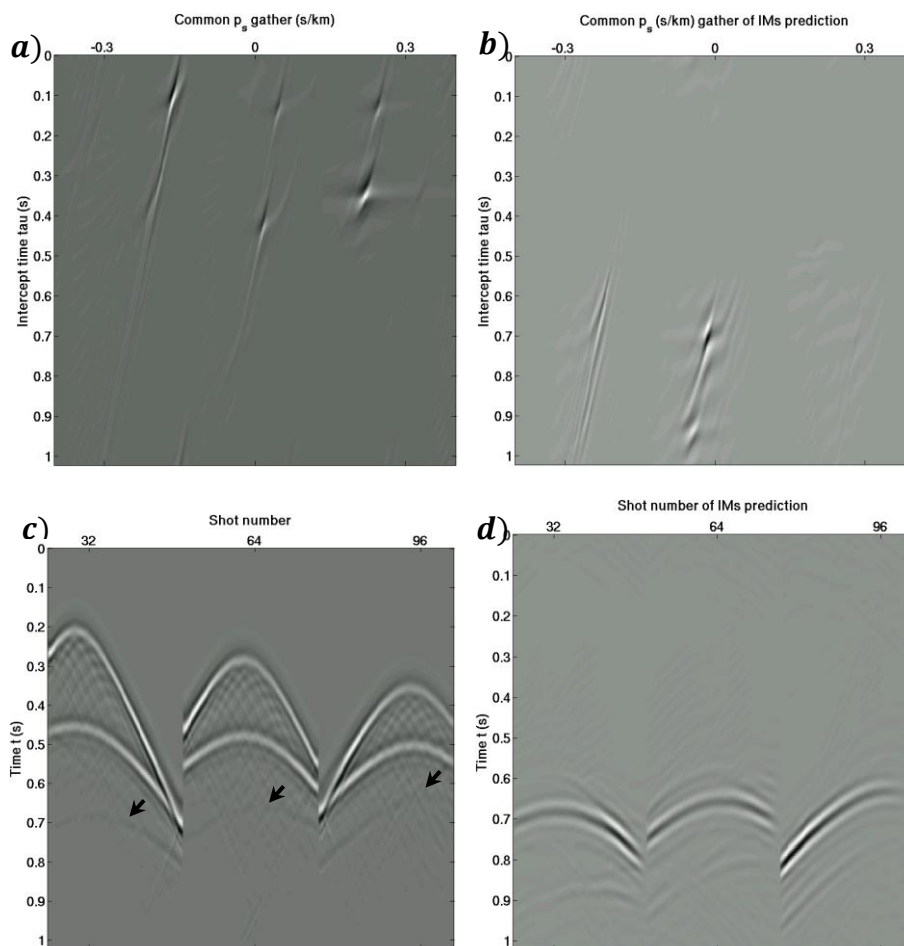


FIG. 11. Internal multiple predictions shown in (p_s, p_g, τ) domain (x_s, x_g, t) domain. a) Common p_s gathers ($p_s = -0.3, 0, 0.3$) extracted from raw data. b) Common p_s gathers ($p_s = -0.3, 0, 0.3$) extracted from predicted results. c) Shot gathers shown at three locations: **310m, 630m, and 950m**. d) Internal multiple predictions in shot gathers at same locations shown in Figure 11c).

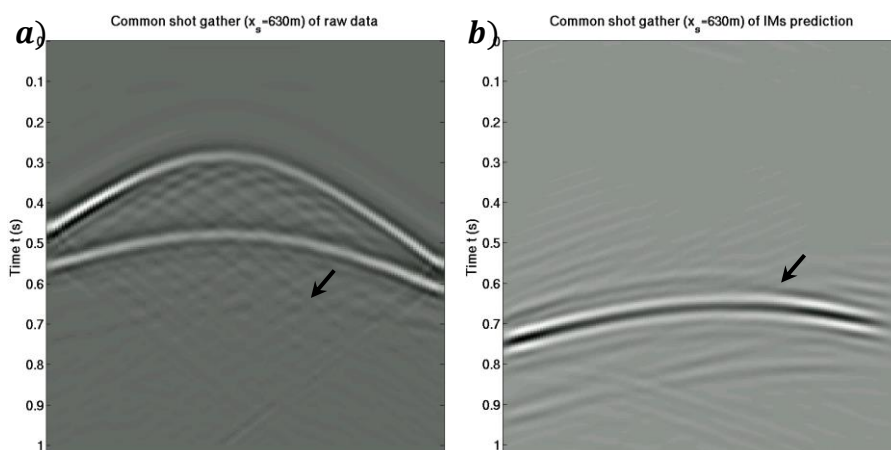


FIG. 12. Comparison between raw data and internal multiples prediction in (x_s, x_g, t) domain. a) Common shot gather of raw data at location: **630m**. b) Common shot gather of IMs prediction at location: **630m**.

Internal multiples predictions were implemented in double $p_s - p_g - \tau$ domain using Eq. (3), and an inverse double $\tau - p$ transform was applied to transfer the prediction to source-receiver coordinates. The 3D view of prediction results are shown in Figure 10.

In Figure 11, we indicate common p_s/p_g gathers and common shot gathers extracted from both raw data and predicted results. Figure 11a) shows common p_s gathers with $p_s = -0.3, 0, 0.3$ extracted from the raw data. Similarly, common p_s gathers with $p_s = -0.3, 0, 0.3$ were also extracted from predicted results and presented in Figure 11b). The predictions in $p_s - p_g - \tau$ domain shows that internal multiple data volume is symmetric over diagonal of matrix (p_s, p_g) which is collocated with the raw data volume. In Figure 11c) and 11d), we compared the raw shot gathers and internal multiple predictions at three locations: 310m, 630m and 950m.

To give an eye on details of predicted traveltimes, common shot gather at location of 630m were extracted from raw data and IMs prediction, shown in Figure 12. The comparison indicates that the internal multiples reconstructed using inverse scattering series algorithm in double plane wave domain shows good agreements with raw dataset. Further study and analysis are still ongoing. Even that, those preliminary tests exemplified the inverse scattering series algorithm in plane wave domain can be a processing tool for internal multiple attenuation with great potential.

CONCLUSIONS

Inverse scattering series algorithm can be applied to reconstruct all possible internal multiples. It can bring more benefits because its' full data driven property and all multiple generators will be treated in a stepwise and automatic way. A double $\tau - p_s - p_g$ transform is introduced to preparing the input for the ISS algorithm. Compared to the wavenumber pseudo-depth domain ISS algorithm, data preparing in double plane wave domain can be presented in a more conveniently and concise manner. In addition to that, after $\tau - p_s - p_g$ transform, the 3D input matrices are more focused along the anti-diagonal planar plane, and can be treated as the anti-diagonal sparse matrices in the processing of prediction, which can reduce the computation burden to some extent. Ultimately, finite difference synthetic gathers were used to examine ISS algorithm and some preliminary results were obtained.

ACKNOWLEDGEMENTS

This work was funded by CREWES industrial sponsors and NSERC (Natural Science and Engineering Research Council of Canada) through the grant CRDPJ 461179-13. The authors thank the sponsors of CREWES for continued support. We also thank Hong Xu for all discussion we made. All CREWES personnel researchers would be grateful acknowledged.

REFERENCES

- Araujo, FV, AB Weglein, PM Carvalho, and RH Stolt. 1994. "Inverse Scattering Series for Multiple Attenuation: An Example with Surface and Internal Multiples." *SEG Annual Meeting*, 1039-41.
- Berkhout, A. J. 2006. "Seismic Processing in the Inverse Data Space." *Geophysics* 71 (4): A29. doi:10.1190/1.2217727.

- Berkhout, A. J., and D. J. Verschuur. 2005. "Removal of Internal Multiples with the Common-Focus-Point (CFP) Approach: Part 1 — Explanation of the Theory." *Geophysics* 70 (3): V45–60. doi:10.1190/1.1925753.
- Coates, R T, A B Weglein, Arco Exploration, and Production Technology. 1996. "Internal Multiple Attenuation Using Inverse Scattering: Results from Prestack 1 & 2D Acoustic and Elastic Synthetics." *SEG Abstracts*, no. 4: 1522–25.
- Diebold, John B., and Paul L. Stoffa. 1981. "The Traveltime Equation, Tau-P Mapping, and Inversion of Common Midpoint Data." *Geophysics* 46 (3): 238–54. doi:10.1190/1.1441196.
- Hernandez, Melissa, Kris Innanen, and Joe Wong. 2012. "Inverse scattering internal multiple attenuation: Implementation on synthetic data and physical mode data."
- Innanen, Kris. 2012. "1 . 5D Internal Multiple Prediction in MATLAB." *CREWES Research Report* 24 (2): 1–7.
- Kelamis, Panos G., Kevin E. Erickson, Dirk J. Verschuur, and A. J. Berkhout. 2002. "Velocity-Independent Redatuming: A New Approach to the near-Surface Problem in Land Seismic Data Processing." *The Leading Edge*, 730–35. doi:10.1190/1.1503185.
- Liu, Faqi, Mrinal K. Sen, and Paul L. Stoffa. 2000. "Dip Selective 2-D Multiple Attenuation in the Plane-wave Domain." *Geophysics* 65 (1): 264–74. doi:10.1190/1.1444717.
- Luo, Yi, Weihong Zhu, Panos G Kelamis, and Saudi Aramco. 2007. "Internal Multiple Reduction in Inverse-Data Domain." *SEG Annual Meeting*, no. 2006: 2485–89.
- Ma, Jitao, Mrinal K. Sen, and Xiaohong Chen. 2009. "Free-Surface Multiple Attenuation Using Inverse Data Processing in the Coupled Plane-Wave Domain." *Geophysics* 74 (4). doi:10.1190/1.3137059.
- Nita, BG, and AB Weglein. 2009. "Pseudo-Depth / Intercept-Time Monotonicity Requirements in the Inverse Scattering Algorithm for Predicting Internal Multiple Reflections 1 Introduction." *Communications in Computational ...* 5 (1): 163–82.
- Ocola, L C. 1972. "A Nonlinear Least-Squares Method for Seismic Refraction Mapping - Part II: Model Studies and Performance of Reframap Method." *Geophysics* 37 (02): 273–87.
- Pan, Pan. 2015. "1.5D Internal Multiple Prediction: An Application on Synthetic Data, Physical Modelling Data and Land Data Synthetics." University of Calgary.
- Pan, Pan, and Kris Innanen. 2013. "Numerical Analysis of 1 . 5D Internal Multiple Prediction." *CREWES Research Reports* 25: 1–12.
- Stoffa, Paul L., Mrinal K. Sen, Roustam K. Seifoullaev, Reynam C. Pestana, and Jacob T. Fokkema. 2006. "Plane-Wave Depth Migration." *Geophysics* 71 (6): S261–72. doi:10.1190/1.2357832.
- Sun, Jian. "1 . 5D Internal Multiple Prediction in Plane Wave Domain."
- Sun, Jian, and Kris Innanen. 2014. "1 . 5D Internal Multiple Prediction in the Plane Wave Domain." *CREWES Research Report* 26: 1–11.
- Taner, M.T. 1980. "Long Period Sea-Floor Multiples and Their Suppression." *Geophysical Prospecting*, no. June 1975: 30–48.
- Treitel, Sven, P. R. Gutowski, and D. E. Wagner. 1982. "Plane-wave Decomposition of Seismograms." *Geophysics* 47 (10): 1375–1401. doi:10.1190/1.1441287.
- Verschuur, D. J., and A. J. Berkhout. 2005. "Removal of Internal Multiples with the Common-Focus-Point (CFP) Approach: Part 2 — Application Strategies and Data Examples." *Geophysics* 70 (3): V61–72. doi:10.1190/1.1925753.
- Verschuur, Dirk Jacob. 1991. "Surface Related Multiple Elimination- an Inversion Approach."
- Weglein, AB, FA Gasparotto, PM Carvalho, and RH Stolt. 1997. "An Inverse-Scattering Series Method for Attenuating Multiples in Seismic Reflection Data." *Geophysics* 62 (6): 1975–89.